Coupled ATP and DNA binding of adeno-associated virus Rep40 helicase

ARTICLE *in* BIOCHEMISTRY · FEBRUARY 2007

Impact Factor: 3.02 · DOI: 10.1021/bi061762v · Source: PubMed

6 AUTHORS, INCLUDING:

Patrick Needham
University of Pittsburgh
14 PUBLICATIONS **152** CITATIONS

SEE PROFILE

Coupled ATP and DNA Binding of Adeno-Associated Virus Rep40 Helicase†

Susan S. Dignam, Roy F. Collaco, Jacob Bieszczad, Patrick Needham, James P. Trempe, and John David Dignam*

Department of Biochemistry and Cancer Biology, University of Toledo College of Medicine, 3035 Arlington Avenue, Toledo, Ohio 43614-5804

Received August 25, 2006; Revised Manuscript Received November 3, 2006

ABSTRACT: Adeno-associated virus 2 Rep40 helicase is involved in packaging single-stranded genomic DNA into virions. ATPase activity was stimulated 5−10-fold by DNA, depending upon assay conditions. The concentration dependence of Rep40 ATPase activity in the absence and presence of DNA indicates that the monomer is inactive and that the active enzyme is at least a dimer. Binding to oligonucleotides, examined by fluorescence anisotropy, was positively cooperative and required ATP or ATPγS; ADP and AMPPCP did not promote binding. The cooperativity and the nucleotide requirement were also demonstrated by surface plasmon resonance. Although the Rep40 behaves as a monomer in solution, it binds to DNA as an oligomer. The requirement of a nucleotide for DNA binding and the stimulation of ATPase activity by DNA indicate that the two processes are linked. Glutaraldehyde cross-linking generated a species that migrates as a trimer on sodium dodecyl sulfate (SDS) gel electrophoresis; ATPγS promoted the formation of this species and higher order oligomers. The predominant cross-linked species was a trimer in the absence of ATPγS, regardless of whether duplex or single-stranded DNA was present. In the presence of duplex or single-stranded DNA and ATPγS, glutaraldehyde cross-linking generated a species that behaved as a dimer on SDS gel elctrophoresis. Sucrose-gradient velocity sedimentation of Rep40 gave an $S_{20,w}$ of 3 in the absence of ligands or in the presence of a 26 bp duplex DNA. The $S_{20,w}$ was 3.5 in the presence of ATPγS and 7 and 7.6 in the presence of DNA and ATPγS.

Adeno-associated virus 2 (AAV2) is a member of the Parvoviridiae, a family of small single-stranded DNA viruses (*1*, *2*); it requires helper functions from another virus for efficient replication of its genome (*3*−*5*). The genome encodes the capsid proteins and four replication proteins: Rep78, Rep68, Rep52, and Rep40, which are SF3-type DNA helicases (*6*−*8*). The mRNAs encoding Rep78/68 and Rep52/40 are synthesized from two promoters such that Rep78 and Rep68 have an N-terminal, sequence-specific DNA-binding domain (*9*) that is absent in Rep52 and Rep40. Rep78 and Rep52 have an additional 92-residue domain in their C termini in place of 9 residues in Rep68 and Rep40 as a result of differential splicing. Rep68 and Rep78 bind specifically to an inverted terminal repeat element (ITR) on the 3′ and 5′ ends of the viral DNA, where they cleave a site specifically to generate a priming site for initiation of the synthesis of a complementary strand. Rep52 and Rep40 are implicated in packaging the single-stranded genomic DNA into virion particles (*10*, *11*) but do not bind to a specific DNA sequence.

Activation of the ATPase activity of Rep68 and Rep78 is associated with oligomerization (*12*, *13*), which is promoted by binding to the target DNA sequence or by high protein concentrations. While some studies indicate that occupation of the nucleotide binding site influences binding to target DNAs (*12*), occupation of the nucleotide binding site is not obligatory and a mutant in this site that eliminates the ATPase activity binds to the inverted terminal repeat. Rep40 also has ATPase activity that is activated by DNA, but there is no sequence specificity in the activation. James et al. (*14*) proposed a hexameric structure for Rep40 based on the similarity of the crystal structure of the monomer to the structures of polyoma and SV40 T antigen monomers. However, presently, no structural data on Rep40 supports this model directly. To understand how Rep40 interacts with ligands and assembles into an active complex, we have examined the requirements for activation of the ATPase of Rep40 and for binding to DNA. Our results indicate that the Rep40 monomer is virtually inactive as an ATPase; assembly to the active species is promoted by binding to DNA. Binding to DNA is in turn linked to the binding of the nucleotide.

EXPERIMENTAL PROCEDURES

Materials. Reduced nicotinamide adenine dinucleotide (NADH), phospho(enol)-pyruvate, ATP, lactate dehydrogenase, pyruvate kinase, and sheared salmon sperm DNA (1000 bp average length) were from Sigma. Q-Sepharose and Superose 12 were from Pharmacia. BioSep-SEC-S 3000 (30 × 0.46 cm) was from Phenomenex. Fluorescein- and biotin-modified oligonucleotides were from Invitrogen or IDT and were purified by reverse-phase high-performance liquid chromatography. Adenosine 5′-*O*-(3-thiotriphosphate) (ATPγS) was from Calbiochem. Common salts and reagents were obtained from various suppliers.

* To whom correspondence should be addresed: Department of Biochemistry and Cancer Biology, University of Toledo College of Medicine, 3035 Arlington Ave., Toledo, OH 43614-5804. Telephone: 419-383-4136. E-mail: david.dignam@utoledo.edu.

† This work was supported by National Institutes of Health Grants AI51471 and GM64765 to J.P.T. and National Institutes of Health Shared Instrumentation Grant PAR-02-036 for the acquisition of the Biacore 3000 plasmon resonance instrument.

10.1021/bi061762v CCC: $37.00
Published on Web 12/15/2006

Oligonucleotides. Duplex oligonucleotides used in this study were prepared by heating equimolar concentrations of complementary DNAs at 100−200 μM in 20 mM Tris-Cl (pH 7.5), 100 mM NaCl, and 1 mM ethylenediaminetetraacetic acid (EDTA), to 100 °C and cooling to room temperature over 3−4 h. The sequences of the oligonucleotides used in this work were derived from elements of the inverted terminal repeat structure of AAV2. The sequences of the biotin- and fluorescein-modified oligonucleotides are given in the Supporting Information.

ATPase Assays. ATPase activity was determined spectrophotometrically; MgADP production was coupled to the pyruvate kinase and lactate dehydrogenase reactions (*15*, *16*). Reaction mixtures contained 50 mM Tris-HCl (pH 7.5), 2 mM $MgCl_2$, 0.1 mg/mL bovine serum albumin, 1 mM MgATP, 1 mM phospho(enol)pyruvate, 0.2 mM NADH, 25 units/mL pyruvate kinase, and 29 units/mL lactate dehydrogenase. Assays were performed with or without added DNA as indicated in the figure captions. In some experiments, sodium chloride and pH were changed as indicated in the figures. Reactions were initiated by the addition of the enzyme, and absorbance at 340 nm was monitored with a Beckman DU640 spectrophotometer at 30 °C. ATPγS was evaluated as the substrate by incubating reaction mixtures with this nucleotide and Rep40 but without the coupling enzymes; after time intervals were varied, coupling enzymes were added to convert the ADP formed to ATP, with accompanying oxidation of NADH. The NADH concentration was determined from the absorbance at 340 nm, using the extinction coefficient of 6.22 mM^{-1} cm^{-1}. One unit is the amount of enzyme that converts 1 nmol of ATP to ADP and P_i per minute.

Glutaraldehyde Cross-Linking of Rep40. Rep40 (0.5 mg mL^{-1}) in 20 mM MOPS-NaOH (pH 7.5), 2 mM $MgCl_2$, 0.5 mM dithiothreitol (DTT), and 0.2 mM EDTA was incubated with 0.005% glutaraldehyde for 10 min at 22 °C. The concentration of glutaraldehyde was chosen, on the basis of experiments where its concentration was varied, so that distinct bands could be detected upon sodium dodecyl sulfate (SDS) gel electrophoresis. Excessive cross-linking at high glutaraldehyde concentrations resulted in most of the protein forming aggregates that did not enter the gel. The reactions were quenched by the addition of sample buffer for SDS gel electrophoresis. Samples were analyzed on 10% acrylamide−bisacrylamide SDS gels.

SDS Polyacrylamide Gel Electrophoresis. Samples were treated with SDS (1%) and mercaptoethanol (5%), subjected to electrophoresis on 10% acrylamide−bisacrylamide (30:1) gels (*17*), and stained with Coomassie Blue R250.

Purification of Rep40. Rep40 was expressed in *Escherichia coli* (BL21DE3star) harboring plasmid pRep40 in pET9a. Cells were grown in Zubay's media (5.6 g/L KH_2PO_4, 28.9 g/L K_2HPO_4, 10 g/L yeast extract, and 1% glucose) (*18*) containing ampicillin (100 μg/mL). Cells were grown in 8 L batches in a 10 L glass carboy at 37 °C to an A_{600} of 0.5−0.6; isopropyl-β-D-thiogalactopyranoside was added to 0.2 mM, and cells were harvested after 3 h and stored at −70 °C. Preparation of the extract and the initial steps were performed at 0−4 °C. Partially thawed cell pellets (approximately 100 g) were broken into pieces and suspended with a Dounce homogenizer in 8 volumes (800 mL) of 50 mM Tris-Cl (pH 7.5 at 25 °C), 10% (v/v) glycerol, 0.1% (v/v) Triton X-100, 2 mM EDTA, 1 mM DTT, 1 mM phenylmethylsulfonyl fluoride, and 0.01 mg/mL egg white lysozyme. The extract was subjected to centrifugation for 30 min at 20000g_{av}. Polyethylene glycol 8000 [0.175 volumes, relative to the supernatant fraction, of a 50% (w/v) solution] was added, with stirring, to the supernatant, stirred for 30 min, and subjected to centrifugation (20000g_{av} for 30 min). The supernatant was retained, and polyethylene glycol 8000 [0.49 volumes, relative to the initial supernatant fraction, of a 50% (w/v) solution] was added and stirred for 30 min. The precipitate was collected by centrifugation (20000g_{av} for 30 min). The pellet was dissolved in 150 mL of 20 mM Tris-Cl (pH 7.5), 20% glycerol (v/v), 40 mM NaCl, 0.5 mM EDTA, and 1 mM DTT with a Dounce homogenizer. The sample was applied at 50 mL/h to Q-Sepharose (2.5 × 14.5 cm), equilibrated in the same buffer. The unbound material (200 mL) was concentrated in an Amicon ultrafiltration cell using a PM10 membrane to 30 mL. Rep40 precipitated during the course of the concentration and was collected by centrifugation; most of the contaminants remained in solution. The precipitate was suspended in 10 mL of 20 mM Tris-Cl (pH 7.5), 10% (v/v) glycerol, 200 mM NaCl, 0.5 mM EDTA, and 1 mM DTT. This material was applied as 0.7 mL aliquots to a Superose 12 gel-filtration column (1 × 32 cm, Pharmacia), equilibrated in 20 mM Tris-Cl (pH 7.5), 10% (v/v) glycerol, 0.2 M NaCl, 0.5 mM DTT, 2 mM $MgCl_2$, and 0.2 mM EDTA. Chromatography was performed at room temperature at 0.5 mL/min; fractions were collected and immediately placed on ice. Fractions were assayed for ATPase activity and examined by SDS polyacrylamide gel electrophoresis. Rep40-containing fractions from multiple runs were combined, concentrated with Vivaspin 6 mL capacity concentrators (10 000 MWCO), and stored at −70 °C as small aliquots. On the basis of SDS gel electrophoresis, the preparations were 90% pure. Rep40 with a Lys to His mutation in the nucleotide binding site (Rep40PNB) was purified as a polyHis-tagged protein by successive chromatography on Ni−NTA Sepharose and Superose 12 as previously described (*19*).

Fluorescence Anisotropy. Fluorescence anisotropy was measured with a PTI QM4 fluorometer equipped with film polarizers. Anisotropy, determined from measurements of fluorescence intensity of the parallel (I_{VV}) and perpendicular (I_{VH}) components, was calculated from the relationship

$$r = \frac{I_{VV} - GI_{VH}}{I_{VV} + 2GI_{VH}}$$

where G is a factor to correct for the difference in the sensitivity of the system to vertically and horizontally polarized light (*20*). Values for anisotropy were derived from the average of 10 measurements of I_{VV} and I_{VH} made at 22 °C. Rep40 was added to reactions containing 20 mM HEPES-NaOH (pH 7.5), 1.0 mM DTT, 1 mM $MgCl_2$, 0.05 mg/mL acetylated bovine serum albumin, 1.0% (v/v) glycerol, and 1 mM Mg·ATPγS as indicated; the NaCl concentration is indicated in the figure captions. Fluorescein-labeled oligonucleotides were present at the indicated concentrations. Samples were equilibrated for 5 min prior to taking measure-

ments. The excitation wavelength was 490 nm, and the emission wavelength was at 515 nm.

Surface Plasmon Resonance. Measurements of the surface plasmon resonance (*21*, *22*) were made with a Biacore 3000 instrument. Oligonucleotides containing 5′-linked biotin were immobilized on streptavidin-coated surfaces in 10 mM HEPES-NaOH at pH 7.4, 150 mM NaCl, 3 mM EDTA, and 0.005% surfactant P20 at 5 μL/min. The level of immobilization was 5−6 response units (RU) per 1000 molecular weight, corresponding to 4−5 fmol/mm^2 using the relationship between the response and mass of 0.8 response unit/pg for nucleic acids (*23*). One surface lacking the oligonucleotide was used as a reference to subtract the background signal.

To bind Rep40 to the immobilized oligonucleotides, the sensor chips were equilibrated in 25 mM HEPES-NaOH at pH 7.0, 50 mM NaCl, 2 mM $MgCl_2$, 1 mM DTT, and 0.005% surfactant P20. The compositions of the running buffer and the buffer containing Rep40 were matched to avoid artifacts resulting from a difference in the bulk refractive index. Rep40 was diluted into the same buffer, and 1 mM ATP or ATPγS was added immediately before injection. The flow rate was 5 μL/min, and the temperature was 25 °C. The Rep40 concentration was varied as indicated in the figures; a total of 35−40 μL of each concentration was injected over the surface, and the response was recorded. The surface was regenerated by a 1 min injection of 0.05% SDS, followed by the running buffer, until the response returned to the starting value. Data were analyzed with BiaEvaluation software version 4.1.

Sucrose-Gradient Velocity Sedimentation. Rep40 alone or Rep40 with ligands (1 mM ATPγS, 4 μM A-stem, or 1 mM ATPγS plus 4 μM A-stem) in 25 mM Tris-HCl (pH 7.5), 25 mM NaCl, 2 mM magnesium chloride, 0.2 mM EDTA, and 1 mM DTT was incubated for 30 min on ice. Samples of 100 μL were loaded on 2 mL gradients of 6−20% (w/v) sucrose in 25 mM Tris-HCl (pH 7.5), 25 mM NaCl, 0.2 mM EDTA, and 1 mM DTT; where appropriate, gradients also contained the ligand at the same concentration present in the sample. Molecular-weight markers human hemoglobin ($S_{20,w}$, 4.3; MW, 64 500) and alcohol dehydrogenase (S_{20w}, 7.4; MW, 141 000) in the same buffer were loaded on a separate gradient. Gradients were centrifuged in a TLS-55 rotor in a Beckman TLX ultracentrifuge at 42 000 rpm (117000g_{av}) for 16 h at 4 °C and fractionated from the top. Fractions were assayed for ATPase in the presence of 0.125 mg/mL sheared salmon sperm DNA and analyzed by SDS gel electrophoresis. Alcohol dehydrogenase was assayed spectrophotometrically; hemoglobin was determined by absorbance at 418 nm.

Size-Exclusion Chromatography. Samples of Rep40 were chromatographed in the absence of nucleotide or in the presence of 1 mM ATP or 0.2 or 0.4 mM ATPγS on a Phenomenex BioSep-SEC-3000 column (4.6 × 300 mm; fractionation range, 5000−700 000 Da). The flow rate was 0.3 mL/min, and absorbance was monitored at 290 nm. Gel-filtration standards from Bio-Rad contained thyroglobulin (MW, 670 000; R_s, 8.5 nm), bovine γ-globulin (MW, 158 000; R_s, 5.1 nm), chicken ovalbumin (MW, 44 000; R_s, 3.2 nm), equine myoglobin (MW, 17 000; R_s, 2.3 nm), and vitamin B_{12} (MW, 1350).

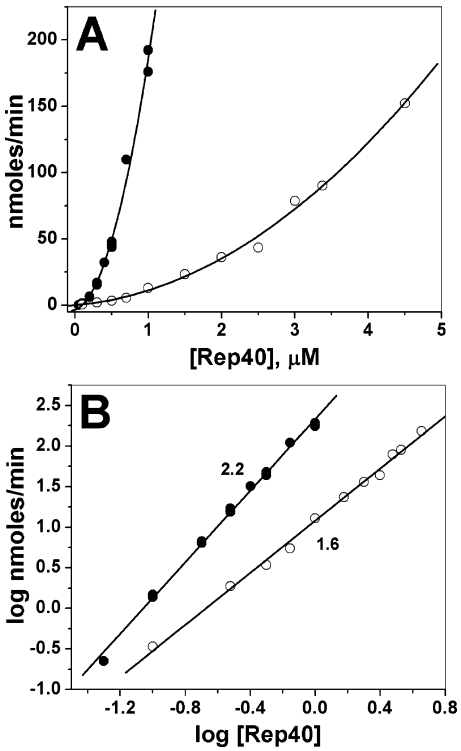

FIGURE 1: Concentration dependence of the ATPase activity and activation by DNA. (A) Rep40 was assayed at the indicated concentrations in the absence (○) or presence (●) of 0.5 mg/mL salmon sperm DNA. The lines are fits of a polynomial to the data. (B) Double log plot of the data in A. The lines are linear fits to the data. The slopes of the lines are indicated.

RESULTS

Activation of Rep40 ATPase Activity. The ATPase activity of Rep40 in the absence of DNA has a characteristic concentration dependence demonstrated in parts A and B of Figure 1. There is an at least second-order dependence on the enzyme concentration in the presence or absence of salmon sperm DNA. The magnitude of the stimulation depends upon the enzyme concentration. These results indicate that the active ATPase must be a dimer or higher order oligomer and that the presence of DNA favors the active oligomeric state. The monomer is either inactive or far less active than the oligomeric form. Activation is not sequence-dependent because sheared salmon sperm DNA and duplex oligonucleotides with different sequences at the same concentration stimulated ATPase activity to the same extent.

To characterize the ATPase, we examined the effect of solution conditions on the magnitude of stimulation by DNA. In the absence of DNA, the enzyme is active from pH 5 to 9; activity was 2.5 times higher at pH 8.5 than at 5.5 (○ in Figure 2A). The pH dependence of ATPase in the presence of DNA was clearly different, with a broad optimum between pH 6.5 and 7 (● in Figure 2A). The result is consistent with the activation being dependent upon two ionizable groups, one with a pK_a in the range of 5.5−5.8 and a second with a pK_a in the range of 7.5−8. The dependence of activation on the ionic strength was also different for activity in the absence and presence of DNA as shown in Figure 2B. In the absence of DNA, activity decreased 2-fold between 0 and 200 mM NaCl, while in the presence of DNA, activity decreased 10-fold until it was the same as the activity in the absence of DNA. The dependence of activation on the ionic strength

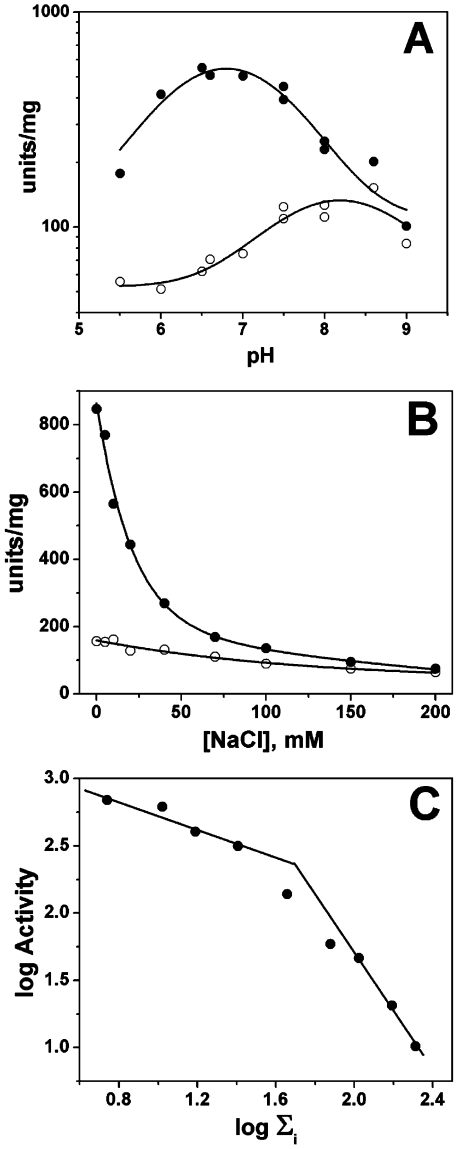

FIGURE 2: Effect of pH and ionic strength on ATPase activity and activation by DNA. The concentration of Rep40 was 180 nM, and the concentration of salmon sperm DNA was 0.125 mg/mL in all assays. (A) Assays were performed at the indicated pH values in the absence (○) or presence (●) of DNA. Buffers used were pH 5.5−6.5, 50 mM MES-NaOH; pH 6.6−8.0, 50 mM HEPES-NaOH; and pH 7.5−9.0, 50 mM Tris-HCl. Ionic strength was kept constant with NaCl. (B) Assays were performed at the indicated concentrations of NaCl in the absence (○) or presence (●) of DNA. (C) Difference between the activity in the presence and absence of DNA in B is shown as a function of the ionic strength.

(Figure 2C) indicates two components, one associated with the displacement of 0.5 ions/mol and a second associated with the displacement of 2 ions/mol.

DNA Binding Properties of Rep40. Rep40 binding to DNA was examined by fluorescence anisotropy as shown in Figure 3 for a 32-nucleotide duplex DNA. Binding of Rep40 to single- or double-stranded fluorescein-labeled oligonucleotides was accompanied by a significant change in the anisotropy that required ATP or ATPγS and was dependent upon the concentration of the oligonucleotide. Because ATPγS is a poor substrate (data not shown), giving values for activity 10−20-fold lower than ATP, we employed this nucleotide in binding assays. The dependence of anisotropy on the DNA concentration is consistent with the protein

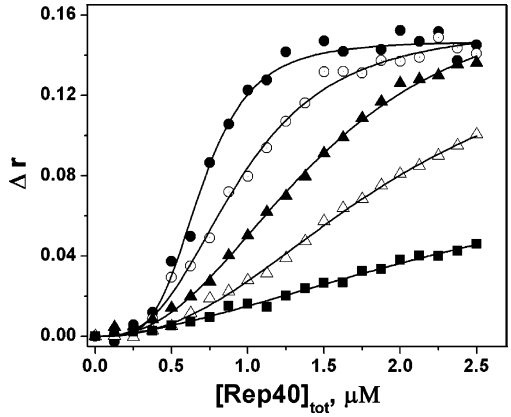

FIGURE 3: Binding of Rep40 to DNA. The binding of Rep40 to increasing concentrations of a 32-nucleotide duplex DNA was measured by fluorescence anisotropy. The DNA concentrations are 10 nM (●), 50 nM (○), 100 nM (▲), 200 nM (△), and 500 nM (■). The lines are fits of the data to the Hill equation.

assembling on the DNA. We attempted to analyze Rep40 binding to oligonucleotides of varying lengths, at different concentrations, to construct model-independent binding isotherms and to estimate the site size. As indicated by the concentration dependence of activity (Figure 1) and as other experiments will show later, Rep40 weakly associates over the concentration range at which binding studies were performed. This association precluded the analysis of the data using approaches developed by Bujalowski and Lohman (*24*−*26*) to construct model-independent binding isotherms, inasmuch as the lack of self-association of the protein is a basic assumption in this analysis. Figure 4 shows the ionic strength dependence of binding to duplex and single-stranded 16-mer (Figure 4A) and 32-mer (Figure 4B) oligonucleotides. The binding constants are apparent values obtained by fitting the data with the Hill equation. The results indicate two components to the binding for both single-stranded and duplex oligonucleotides, with both size oligonucleotides. One component results in the release of 0.35−0.37 ions/mol, and a second results in the release of 1.63 (the 32-mer) to 1.83 (the 16-mer) ions/mol, in accordance with the effect of ionic strength on the activation of the ATPase by DNA.

We used plasmon resonance as an independent method to measure binding using biotinylated oligonucleotides immobilized on a streptavidin surface. As shown in Figure 5A for oligo dT_{26}, binding depended upon ATPγS and showed rapid dissociation. In the absence of the nucleotide (Figure 5B), both the association and dissociation phases were slower and the amplitude of the signal was at least an order of magnitude lower. The effect of the nucleotide was seen with oligo dT_{16}, oligo dT_{38}, and a 61-nucleotide oligo containing all four bases (data not shown). The maximum amplitude both in the presence and absence of the nucleotide showed length dependence. ADP and AMPPCP did not promote binding (data not shown). The amplitude in time courses with ATP was approximately 5-fold lower, likely reflecting the fact that ATP is a good substrate compared to ATPγS (data not shown). Rep40 at varying concentrations, with 1 mM ATPγS, was passed over surfaces (Figure 6) with single-stranded (Figure 6A) or duplex (Figure 6B) 32-mer oligonucleotides. The concentration dependence of the maximum amplitude of the signal for these oligonucleotides is shown in Figure 6C. Because the association involves multiple

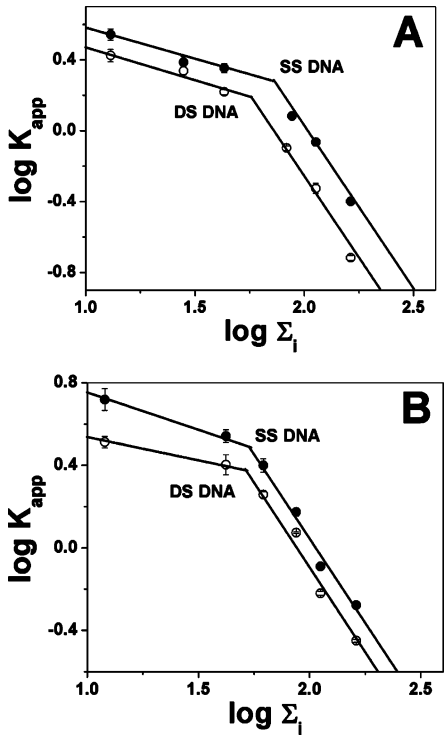

FIGURE 4: Ionic strength dependence of the binding of Rep40 to DNA. The binding of Rep40 to single-strand (●) and duplex (○) 16-nucleotide (A) or 32-nucleotide (B) DNAs was measured by fluorescence anisotropy at the indicated ionic strengths. The concentration of DNA was 50 nM, and Rep40 was varied as in Figure 3. Data were fit to the Hill equation. Values for K_{app} are shown as a function of the ionic strength.

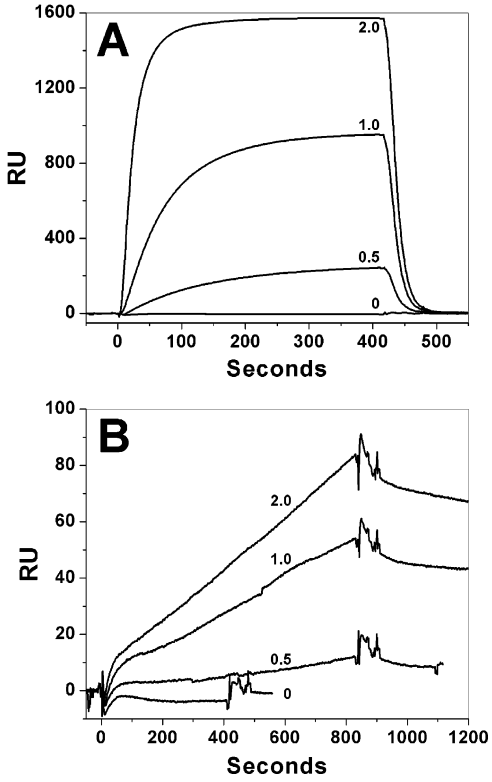

FIGURE 5: Dependence of the binding of Rep40 to DNA on the nucleotide. Binding of Rep40 to immobilized oligo dT_{26} was measured by surface plasmon resonance in the presence (A) or absence (B) of 1 mM ATPγS at the indicated concentrations (in micromolars) of Rep40.

molecules of Rep40 and is not simple Langmuir binding, we did not attempt to model the time course of the association and dissociation. In the instances where the association did not reach a plateau, the amplitude of the plateau was estimated by fitting the time course to two exponentials. The concentration dependence of binding to a single-stranded or duplex 32-mer oligonucleotide in Figure 6C shows evidence of cooperativity. Similar behavior was seen with longer and shorter oligo dT and with single-stranded and duplex oligonucleotides of mixed base composition. The plateau was similar for short duplex and single-stranded oligonucleotides; binding was greater for duplex oligonucleotides versus single strands as the length increased (data not shown). The effect of the length on the binding properties of mixed composition oligonucleotides is shown in Figure 7. The sequences of these oligonucleotides are given in the Supporting Information and are based on elements of the inverted terminal repeat of adeno-associated virus 2. The dissociation constant is greater for the shortest duplex and single-stranded oligonucleotide but is similar for most of the longer oligonucleotides (Figure 7A). The shortest single-strand and duplex oligonucleotides also showed greater cooperativity in binding as reflected in the value of the Hill coefficient (Figure 7B). The stoichiometry determined from the maximum amplitude for binding showed clear length dependence and was greater for duplex than for single-stranded oligonucleotides (Figure 7C). We also examined the dependence of the binding properties with single-stranded oligo dT as shown in Figure 8. There was little dependence of the dissociation constant (Figure 8A) on oligonucleotide length. Binding was more cooperative with shorter oligonucleotides as shown by the effect on the Hill coefficient in Figure 8B. There was a clear dependence of the stoichiometry of binding on oligonucleotide length as shown in Figure 8C. The stoichiometry of binding was higher for oligo dT (compare Figures 7C to 8C) than for the oligonucleotides of mixed composition, indicating that binding is influenced by oligonucleotide composition.

Oligomerization of Rep40. The indication of cooperativity in binding of Rep40 to DNA seen with both anisotropy and surface plasmon resonance and the concentration dependence of ATPase activity are consistent with the Rep protein assembling into an oligomer. We examined the oligomerization of Rep40 in the absence and presence of ligands employing sucrose-gradient sedimentation as shown in Figure 9. In the absence of ligands (Figure 9A), the Rep40 ATPase activity and protein had a $S_{20,w}$ of 3. A slightly higher $S_{20,w}$ value of 3.5 was obtained in the presence of ATPγS (Figure 9A) or a duplex oligonucleotide (Figure 9B). In the presence of ATPγS and DNA, the activity sedimented as two overlapping activity peaks with $S_{20,w}$ values of 7 and 7.6. These results indicate that the enzyme forms a complex (or complexes) with the oligonucleotide and that the formation of complexes requires the nucleotide. As seen in the results of acrylamide gel electrophoresis of sucrose-gradient fractions, most of the protein sedimented at a position corresponding to that of the ATPase activity, indicating that most of the protein in the preparation could form the complex with DNA. When examined by size-exclusion chromatography (data not shown), Rep40 eluted with a retention time corresponding to a monomer, consistent with its behavior

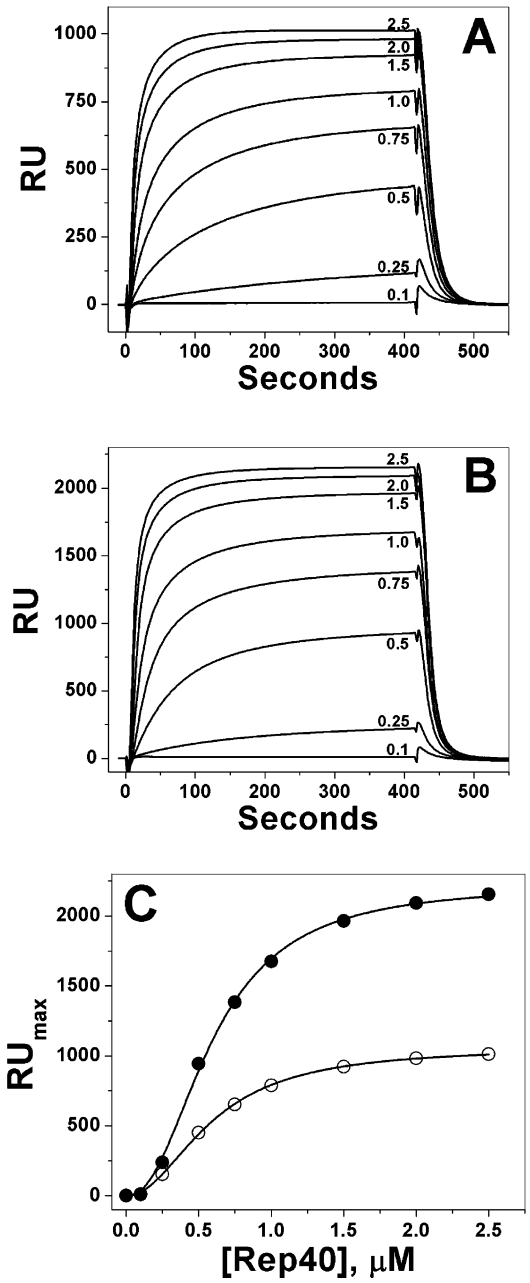

FIGURE 6: Analysis of the binding of Rep40 to DNA by surface plasmon resonance. Sensorgrams were obtained with immobilized single-strand (A) or duplex (B) 32-nucleotide A-stem DNAs at the indicated concentrations (in micromolars) of Rep40. (C) Maximum RU values from the data in A (○, single strand) and B (●, duplex) are shown as a function of the Rep40 concentration. The lines are fits of the Hill equation to the data.

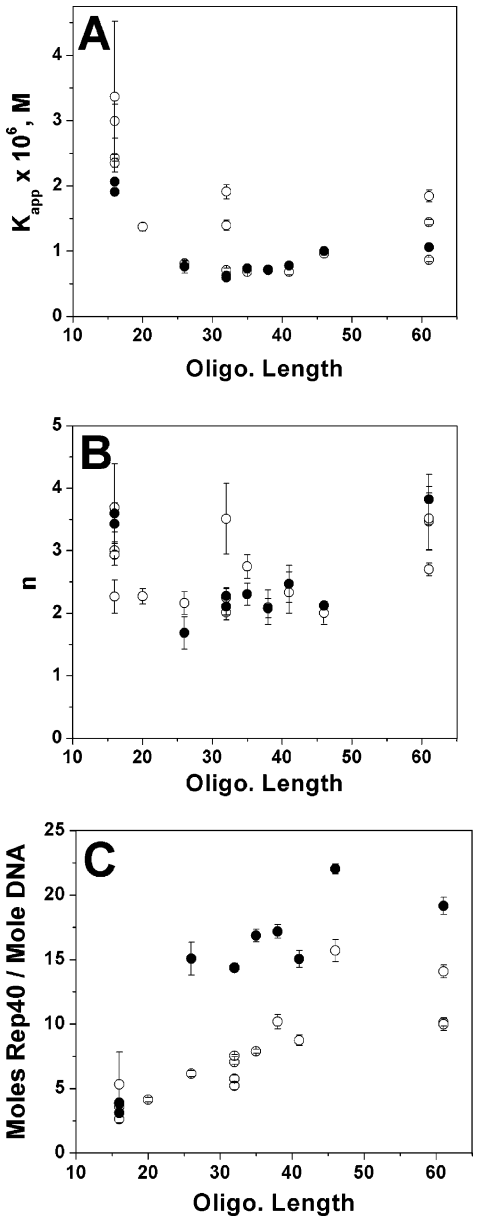

FIGURE 7: Length dependence of the binding of Rep40 to A-stem DNAs. Binding of Rep40 to single-strand (○) and duplex (●) A-stem DNAs of the indicated lengths was measured by surface plasmon resonance, and the data were fit to the Hill equation as in Figure 6. The values for K_{app} (A) and the Hill coefficient n (B) are shown as a function of the length of DNA. Error bars are ± the standard deviation of the fit. (C) Stoichiometry of binding was determined and is shown as a function of the length of DNA.

on sucrose-gradient sedimentation. In the presence of ATPγS, most of the Rep40 still eluted at the retention time of a monomer but with a detectable shoulder corresponding to a slightly larger size (data not shown).

As an alternate method for examining oligomerization, we employed cross-linking with glutaraldehyde as shown in Figure 10A. The major cross-linked product in the absence of ligands migrated on SDS gels at a MW of 105 000, consistent with a trimer of the subunit (MW, 35 000). In the presence of ATP or ATPγS, the amount of this species increased, and with ATPγS, two larger species appeared, migrating at approximately 200 000 and 400 000. In the presence of a molar excess of a 26 bp duplex DNA, the 105 000 MW species was diminished, most notably in the presence of ATPγS. ADP did not promote cross-linking to the same degree as ATPγS. A 70 000 MW species was detected when Rep40 was cross-linked in the presence of ATPγS and DNA; the size of this cross-linked product was the same for oligonucleotides ranging from 25 to 60 bp (data not shown).

The effect of the DNA concentration on oligomerization was examined by glutaraldehyde cross-linking as shown in Figure 10B. With either duplex or single-strand DNA, the amount of both the 105 000 and 70 000 MW species increased as the DNA concentration decreased.

Binding of Rep40PNB. Rep40 with a mutation in the purine nucleotide binding site (K to H, designated Rep40PNB)

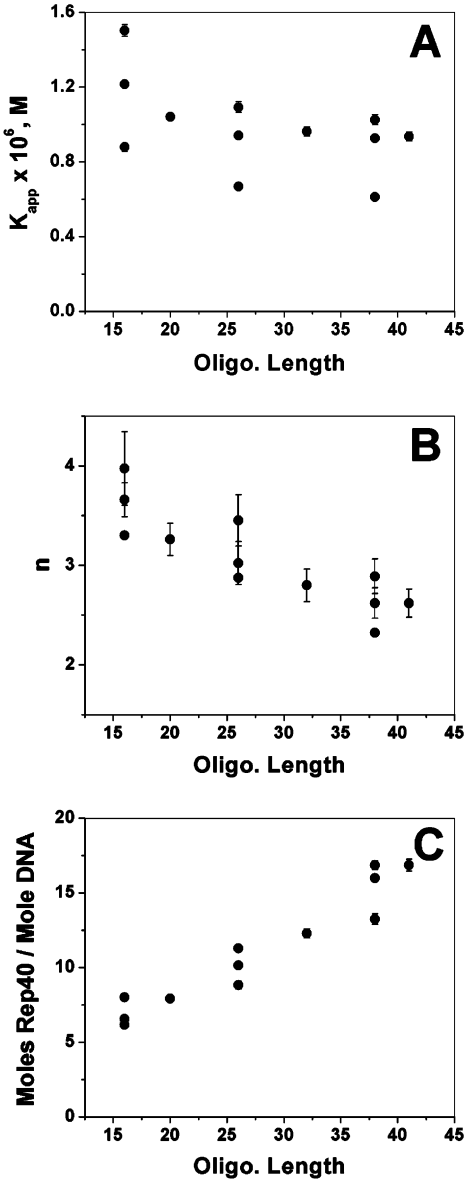

FIGURE 8: Binding of Rep40 to oligo dT. Binding of Rep40 to immobilized oligo dT of the indicated lengths was measured by surface plasmon resonance as in Figure 7. The values for K_{app} (A) and the Hill coefficient n (B) are shown as a function of the length of DNA. Error bars are ± the standard deviation of the fit. (C) Stoichiometry of binding was determined and is shown as a function of the length of DNA.

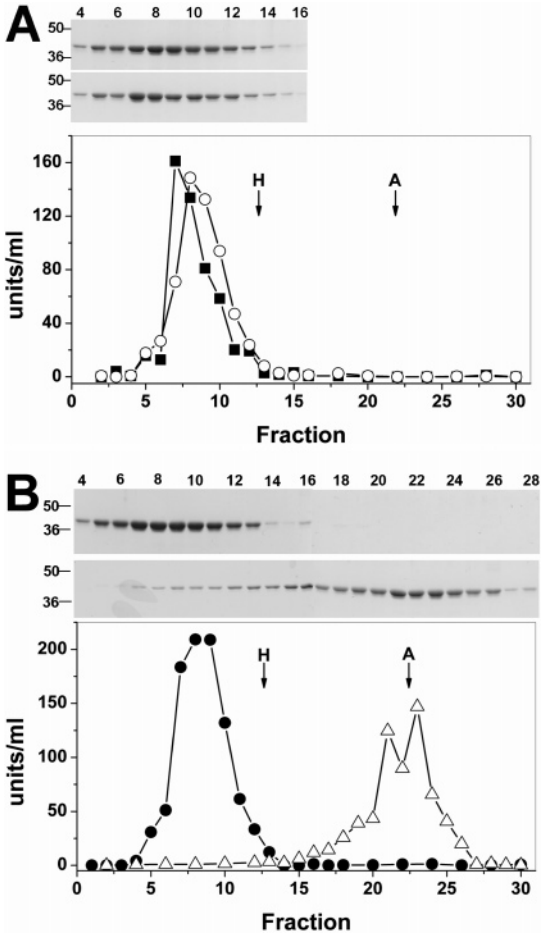

FIGURE 9: Sucrose density gradient sedimentation of Rep40. (A) Rep40 (23 μM) was fractionated on 6−20% (w/v) sucrose density gradients in the absence of ligand (■) or in the presence of 1 mM ATPγS (○). The gradients were fractionated from the top, and fractions were assayed for ATPase in the presence of salmon sperm DNA. Standards were H, hemoglobin (MW, 64 500; $S_{20,w}$, 4.3), and A, alcohol dehydrogenase (MW, 141 000, $S_{20,w}$, 7.4). The inset shows SDS−PAGE analysis of the fractions: upper panel, 1 mM ATPγS; lower panel, no ligand. (B) Rep40 (23 μM) was fractionated on sucrose gradients in the presence of 4 μM A-stem duplex (●) or in the presence of 4 μM A-stem and 1 mM ATPγS (△). The gradients were fractionated and assayed as in A. Standards are the same as in A. The inset shows SDS−PAGE analysis of the fractions: upper panel, A-stem; lower panel, A-stem and ATPγS.

lacks detectable ATPase and helicase activity (*19*). We examined this mutant to determine if it would bind to DNA. No binding was detected in the presence or absence of nucleotides (ATPγS or ATP) by fluorescence anisotropy or surface plasmon resonance (data not shown).

DISCUSSION

Rep40 serves an essential function in the assembly of infectious AAV virions. Analysis of Rep40 mutants with defects in ATPase and helicase activity indicate that it is involved in packaging single-stranded genomic DNA into preformed virions in a 3′ → 5′ direction (*10*, *27*, *28*). This function requires that the enzyme binds to DNA; the present studies indicate that binding is promoted by ATP. The fact that the effect of ATP on DNA binding was not reported in earlier studies (*28*) is likely attributable to the experimental conditions used in the earlier binding studies. Weak binding was detected by plasmon resonance at high Rep40 concentrations, but the kinetics of association and dissociation are different compared to that observed in the presence of ATPγS. Yoon-Robarts et al. (*28*) appear to have fitted the data with a hyperbolic binding isotherm, implying that there was no evidence of cooperativity, which differs significantly from our findings. Their results could be accounted for by the weak binding that we detected in the absence of the nucleotide using plasmon resonance.

The concentration dependence of ATPase activity in the presence or absence of DNA indicates that the protein assembles into the active ATPase and that the monomeric subunits are either inactive or far less active than the oligomer. The reciprocal requirements of the ATPase activity for DNA binding and DNA binding for ATP indicate that the equilibria are linked. The results suggest that ATP induces a conformational change that facilitates DNA binding and

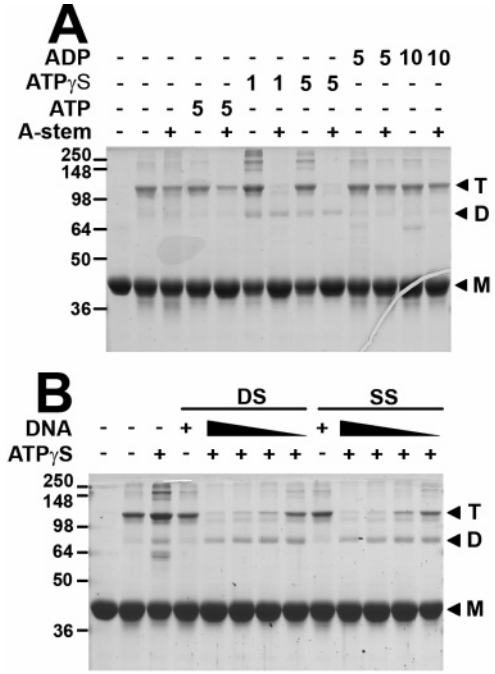

FIGURE 10: Effect of nucleotides and DNA on the cross-linking of Rep40. Rep40 (12.5 μM, 4.5 μg/lane) was incubated with 0.005% glutaraldehyde. (A) Incubation was in the absence or presence of 45 μM A-stem duplex at the indicated concentrations (in millimolars) of nucleotides. The lane next to the markers is Rep40 without glutaraldehyde. (B) Rep40 was incubated with A-stem duplex (DS) or A-stem-2 (SS), from 45 to 1 μM, in the presence of 1 mM ATPγS. The samples without nucleotide were with 45 μM A-stem (DS or SS). The lane next to the markers is Rep40 without glutaraldehyde. The positions of the monomer (M) and the presumptive dimer (D) and trimer (T) are indicated at the right in the figures.

the DNA binding in turn induces a conformational change, perhaps leading to assembly, which activates ATP hydrolysis. The effects of mutations in the nucleotide binding site that eliminate ATPase activity on DNA binding are also consistent with this idea. Oligomerization of SV40 and polyoma T antigens, which, like Rep40, are SF3-type helicases, are affected by ATP and DNA (*29*−*32*), and the assembly of some bacterial helicases are also promoted by ATP (*33*−*37*).

While the oligomeric structure of the active form of Rep40 is still unclear, it must act as an oligomer. The present study and earlier work indicate that Rep40 is a monomer over a range of protein concentrations (*28*) in the absence of ligands. ATPγS causes a small increase in the sedimentation constant and promotes the formation of oligomeric species in glutaraldehyde cross-linking studies corresponding to trimers, hexamers, and higher order oligomers. However, in the presence of ATPγS and DNA, the most abundant cross-linked species corresponds to a dimer. The results of the cross-linking studies suggesting a dimer may be indicative of the interface available for cross-linking rather than an indication of the oligomeric state. One could imagine that tetramers or hexamers are formed but that the subunit contacts are favorable only for the cross-linking of the dimer. However, the sedimentation studies performed to complement the cross-linking did not demonstrate a species corresponding to a hexamer. A hexamer is still a possibility because it might be stabilized by the association with another Rep protein or possibly capsid proteins. Rep proteins do associate with capsids (*10*), and some capsid mutations that block Rep−capsid association block packaging (*10*, *38*, *39*). Although the hexameric structural model proposed for Rep40 (*14*, *40*) is appealing in view of the similarity to the SV40 and polyoma T antigens, it should be viewed with caution because it is not yet supported by rigorous biophysical studies. In addition to forming hexamers and double hexamers (*30*−*32*, *41*), the SV40 T antigen also forms dimers and trimers that may lead to larger oligomers. Similar findings have been reported for bovine papilloma virus E1 protein (*42*, *43*), a SV40 T antigen homologue. The various Rep40 oligomeric species detected by cross-linking and sucrose-gradient sedimentation might reflect different assembly intermediates.

An important question is what is the nature of the conformational change induced by ATP binding? The X-ray structures of the unligated and ADP-ligated forms have been solved, but interestingly, ADP does not support binding to DNA, suggesting that the structure of the ATP−enzyme complex or a complex with a catalytically inert ATP analogue might differ significantly from the ADP complex.

SUPPORTING INFORMATION AVAILABLE

Coupled ATP and DNA binding of adeno-associated virus Rep40 helicase oligonucleotides used for surface plasmon resonance, oligonucleotides used for anisotropy experiments, and oligonucleotides for A-stem. This material is available free of charge via the Internet at http://pubs.acs.org.

REFERENCES

1. Bloom, M. E., and Young, N. S. (2001) *Parvoviruses*, 4th ed., Fields Virology (Knipe, D. M., and Howley, P. M., Eds.) Vol. 2, pp 2361−1379, Lippincott, Williams, and Wilkins, New York.
2. Muzyczka, N., and Berns, K. I. (2001) *Parvoviridiae: The Viruses and Their Replication*, 4th ed., Fields Virology (Knipe, D. M., and Howley, P. M., Eds.) Vol. 2., pp 2327−2359, Lippencott, Williams, and Wilkins, New York.
3. Georg-Fries, B., et al. **(**1984**)** Analysis of proteins, helper dependence, and seroepidemiology of a new human parvovirus, *Virology 134*, 64−71.
4. Berns, K. I., and Bohensky, R. A. (1987) Adeno-associated viruses: An update, *Adv. Virus Res. 32*, 243−306.
5. Schlehofer, J. R., Ehrbar, M., and zur Hausen, H. (1986) Vaccinia virus, herpes simplex virus, and carcinogens induce DNA amplification in a human cell line and suppport replication of a helper virus dpendent parvovirus. *Virology 152*, 110−117.
6. Im, D. S., and Muzyczka, N. (1992) Partial purification of adeno-associated virus Rep78, Rep52, and Rep40 and their biochemical characterization. *J. Virol. 66*, 1119−1128.
7. Snyder, R. O., et al. Features of the adeno-associated virus origin involved in substrate recognition by the viral Rep protein, *J. Virol. 67*, 6096−6104.
8. Wonderling, R. S., et al. (1997) The Rep68 protein of adeno-associated virus type 2 increases RNA levels from the human cytomegalovirus major immediate early promoter, *Virology 236*, 167−176.
9. Owens, R. A., et al. (1993) Identification of a DNA-binding domain in the amino terminus of adeno-associated virus Rep proteins, *J. Virol. 67*, 997−1005.
10. Dubielzig, R., et al. (1999) Adeno-associated virus type 2 protein interactions: Formation of pre-encapsidation complexes, *J. Virol. 73*, 8989−8998.
11. Chejanovsky, N., and Carter, B. J. (1989) Mutagenesis of an AUG codon in the adeno-associated virus *rep* gene: Effects on viral DNA replication, *Virology 173*, 120−128.
12. Li, Z., et al. (2003) Characterization of the adenoassociated virus Rep protein complex formed on the viral origin of DNA replication, *Virology 313*, 364−376.

13. Zhou, X., et al. (1999) Biochemical characterization of adeno-associated virus rep68 DNA helicase and ATPase activities, *J. Virol. 73*, 1580−1590.
14. James, J. A., et al. (2003) Crystal structure of the SF3 helicase from adeno-associated virus type 2, *Structure 11*, 1025−1035.
15. Cook, P. F., et al. (1982) Adenosine cyclic 3′,5′-monophosphate dependent protein kinase: Kinetic mechanism for the bovine skeletal muscle catalytic subunit, *Biochemistry 21*, 5794−5799.
16. Cleland, W. W. (1979) Optimizing coupled enzyme assays, *Anal. Biochem. 99*, 142−145.
17. Laemmli, U. K. (1970) Cleavage of structural proteins during the assembly of the head of bacteriophage T4, *Nature 227*, 680−685.
18. Zubay, G., Chambers, D. A., and Chang, L. C. (1969) A DNA-directed cell-free system for β-galactosidase synthesis; characterization of the de novo synthesized enzyme and some aspects of the regulation of synthesis, *Cold Spring Harbor Symp. Quant. Biol. 34*, 753−761.
19. Collaco, R. F., et al. (2003) A biochemical characterization of the adeno-associated virus Rep40 helicase, *J. Biol. Chem. 278*, 34011−34017.
20. Lakowicz, J. R. (1999) *Principles of Fluorescence Spectroscopy*, 2nd ed., Kluwer Academic/Plenum, New York.
21. Rich, R. L., and Myszka, D. G. (2000) Advances in surface plasmon resonance biosensor analysis, *Curr. Opin. Biotechnol. 11*, 54−61.
22. Karlsson, R. (2004) SPR for molecular interaction analysis: A review of emerging application areas, *J. Mol. Recognit. 17*, 151−161.
23. Fisher, R. J., et al. (2006) Complex interactions of HIV-1 nucleocapsid protein with oligonucleotides, *Nucleic Acids Res. 34*, 472−484.
24. Jezewska, M. J., and Bujalowski, W. (1996) A general method of analysis of ligand binding to competing macromolecules using the spectroscopic signal originating from a reference macromolecule. Application to *Escherichia coli* replicative helicase DnaB protein nucleic acid interactions, *Biochemistry 35*, 2117−2128.
25. Bujalowski, W., and Lohman, T. M. (1987) A general method of analysis of ligand−macromolecule equilibria using a spectroscopic signal from the ligand to monitor binding. Application to *Escherichia coli* single-strand binding protein−nucleic acid interactions, *Biochemistry 26*, 3099−3106.
26. Lohman, T. M., and Bujalowski, W. (1991) Thermodynamic methods for model-independent determination of equilibrium binding isotherms for protein−DNA interactions: Spectroscopic approaches to monitor binding, *Methods Enzymol. 208*, 258−290.
27. King, J. A., et al. (2001) DNA helicase-mediated packaging of adeno-associated virus type 2 genomes into preformed capsids, *EMBO J. 20*, 3282−3291.
28. Yoon-Robarts, M., et al. (2004) Residues within the B′ motif are critical for DNA binding by the superfamily 3 helicase Rep40 of adeno-associated virus type 2, *J. Biol. Chem. 279*, 50472−50481.
29. Herzog, R. W., and High, K. A. (1998) Problems and prospects in gene therapy for hemophilia, *Curr. Opin. Hematol. 5*, 321−326.
30. Gai, D., et al. (2004) Insights into the oligomeric states, conformational changes, and helicase activities of SV40 large tumor antigen, *J. Biol. Chem. 279*, 38952−38959.
31. Gai, D., et al. (2004) Mechanisms of conformational change for a replicative hexameric helicase of SV40 large tumor antigen, *Cell 119*, 47−60.
32. VanLoock, M. S., et al. (2002) SV40 large T antigen hexamer structure: Domain organization and DNA-induced conformational changes, *Curr. Biol. 12*, 472−476.
33. Patel, S. S., and Hingorani, M. M. (1993) Oligomeric structure of bacteriophage T7 DNA primase/helicase proteins, *J. Biol. Chem. 268*, 10668−10675.
34. Picha, K. M., and Patel, S. S. (1998) Bacteriophage T7 DNA helicase binds dTTP, forms hexamers, and binds DNA in the absence of Mg^{2+}. The presence of dTTP is sufficient for hexamer formation and DNA binding, *J Biol. Chem. 273*, 27315−27319.
35. Gogol, E. P., et al. (1992) Cryoelectron microscopic visualization of functional subassemblies of the bacteriophage T4 DNA replication complex, *J. Mol. Biol. 224*, 395−412.
36. Xu, H., et al. (2000) DNA helicase RepA: Cooperative ATPase activity and binding of nucleotides, *Biochemistry 39*, 12225−12233.
37. Niedenzu, T., et al. (2001) Crystal structure of the hexameric replicative helicase RepA of plasmid RSF1010, *J. Mol. Biol. 306*, 479−487.
38. Bleker, S., Sonntag, F., and Kleinschmidt, J. A. (2005) Mutational analysis of narrow pores at the fivefold symmetry axes of adeno-associated virus type 2 capsids reveals a dual role in genome packaging and activation of phospholipase A2 activity, *J. Virol. 79*, 2528−2540.
39. Wu, P., et al. (2000) Mutational analysis of the adeno-associated virus type 2 (AAV2) capsid gene and construction of AAV2 vectors with altered tropism, *J. Virol. 74*, 8635−8647.
40. James, J. A., et al. (2004) Structure of adeno-associated virus type 2 Rep40−ADP complex: Insight into nucleotide recognition and catalysis by superfamily 3 helicases, *Proc. Natl. Acad. Sci. U.S.A. 101*, 12455−12460.
41. Schuck, S., and Stenlund, A. (2005) Assembly of a double hexameric helicase, *Mol. Cell 20*, 377−389.
42. Sedman, J., and Stenlund, A. (1996) The initiator protein E1 binds to the bovine papillomavirus origin of replication as a trimeric ring-like structure, *EMBO J. 15*, 5085−5092.
43. Enemark, E. J., Stenlund, A., and Joshua-Tor, L. (2002) Crystal structures of two intermediates in the assembly of the papillomavirus replication initiation complex, *EMBO J. 21*, 1487−1496.

BI061762V